19

Picosecond Laser Pulse Distortion by Propagation through a Turbulent Atmosphere

Josef Blazej, Ivan Prochazka and Lukas Kral
Czech Technical University in Prague
Czech Republic

1. Introduction

We have been investigating the influence of atmospheric turbulence on the propagation of a picosecond laser pulse. The figure of merit of presented results is the time of propagation, its absolute delay and jitter. Phase wavefront deformation or beam profile changes were not studied. The correlation of the atmospheric turbulence with the propagation delay fluctuation was measured. The research was motivated by the needs of highly precise laser ranging of ground, air, and space objects; and highly precise and accurate time transfer ground-to-space and ground-to-ground by means of picosecond optical laser pulse.
Firstly for comparison, lets briefly summarize the effects of a turbulent atmosphere to continuous laser beam. The total effect of atmospheric turbulences on a continuous laser beam propagation is a highly complex subject. Atmospheric turbulences can be defined as random spatial variations in the refraction index of the atmosphere resulting in a distortion of the spatial phase fronts of the propagating signal. Spatial phase front distortion induces the variable path of light energy and thus all effects described later on. Variations of the refraction index are caused by the turbulent motion of the atmosphere due to the variations in temperature and gradients in the water vapour. Following (Degnan, 1993), the optically turbulent atmosphere produces three effects on low power laser beams: 1) beam wander, 2) beam spread and 3) scintillations. Severe optical turbulence can result in a total beam break-up. Beam wander refers to the random translation of the spatial centroid of the beam and is generally caused by the larger turbulent eddies through which the beam passes. In astronomical community it is usually referred as seeing. Beam spread is a short term growth in the effective divergence of the beam produced by smaller eddies in the beam path. The two effects are often discussed together in terms of a "long term" and "short term" beam spread. The "long term" beam spread includes the effects of beam wander, whereas the "short term" beam spread does not. For more details, see (Degnan, 1993). Maximum turbulence occurs at mid-day in the desert (low moisture) under clear weather conditions. For the usual laser wavelength of 532 nm one can expect 2.4-4.6 cm for the coherence length at zenith angles of 0° and 70° respectively. At the tripled Nd:YAG wavelength (355 nm) the corresponding values are 3.1 and 1.6 cm (Degnan, 1993). Turbulence induced beam spreading will only have a significant impact on beam divergence (and hence signal level) if the coherence length is on the order of, or smaller than, the original effective beam waist radius. Since a typical 150 μrad beam implies an effective waist radius of 2.26 mm, the effect of beam spread on signal level for such systems is relatively small, i.e. a few percent.

Atmospheric turbulence produces a fluctuation in the received intensity at a point detector. During satellite laser ranging aperture averaging, which occurs at both the target retro-reflectors and at the ground receiving telescope, tends to reduce the magnitude of the fluctuations. Thus the round trip propagation geometry must be considered when evaluating theoretical scintillation levels. The effect of scintillation is significant under conditions of strong turbulence.

In contrast with above mentioned, we have been investigating the influence of atmospheric turbulence on the propagation of a picosecond laser pulse. In this case, the fluctuation should be not described as a coherence length, but typically as a time jitter of absolute delay of laser pulse propagated trough the atmosphere. The research was motivated by the needs of highly precise laser ranging of ground, air and space objects. The ground targets laser ranging with picosecond single shot resolution revealed the fact, that the resulting precision in influenced, among others, by the atmospheric index of refraction fluctuations. The influence of the atmospheric refraction index fluctuations on the star image is known for a long time, it is called seeing (Bass, 1992). It has been studied for more than a century. It represents a serious limitation in the astronomical images acquisition. The angular resolution of large astronomical telescope is limited by the seeing, its influence is much larger in comparison to a diffraction limit. Recently, numerous techniques exist for seeing compensation by means of adaptive optics (Roddier, 1998) active and nowadays also passive.

The interesting point of view is the comparison of propagation delay between microwave and optical region. Due to the refractive index and its variations within the troposphere, the microwave signal is also naturally delayed as the optical laser pulse propagated. Typically, the total delay of the radio signal is divided into “hydrostatic” and “wet” components. The hydrostatic delay is caused by the refractivity of the dry gases in the troposphere and by the nondipole component of the water vapour refractivity. The main part, or about 90 % of the total delay, is caused by the hydrostatic delay and can be very accurately predicted for most of the ranging applications using surface pressure data. The dipole component of the water vapour refractivity is responsible for the wet delay and amounts to about 10% of the total delay. This corresponds to 5-40 cm (above 1 ns) for the very humid conditions. The mapping function is used to transform the zenith troposphere delay to the slant direction. In recent years, the so-called Niell Mapping Function served as a standard for processing microwave measurements. It was built on one year of radiosonde profiles primarily from the northern hemisphere (Niell, 1996). Compared to the microwave technique, the main advantages of the SLR measurements are the insensitivity to the first and higher order ionospheric propagation effects, and the relatively high accuracy with which water vapour distribution can be modelled. Ions are too heavy and sluggish to respond to optical frequencies in the 300 to 900 THz band. Laser wavelengths in the visible and ultraviolet bands are typically far from strong absorption feature in the water vapour spectrum. Signal delay due to the water vapour in atmosphere is significantly different in the optical versus the microwave band. The ratio is about 67, meaning that the typical “wet component” in the zenith direction of about 5-40 cm (above 1 ns) for the microwave band (GPS) corresponds to the delay of about 0.1-0.6 cm (2 ps) for optical band. Since the effect is relatively small, about 80 % of the delay can be modelled by means of surface pressure, temperature and humidity measured on the station. Recently GNSS-based measurements offered new and promising possibilities, the global IGS network and dense regional GNSS networks developed all around the world provide high temporal information on the integrated atmospheric water vapour.

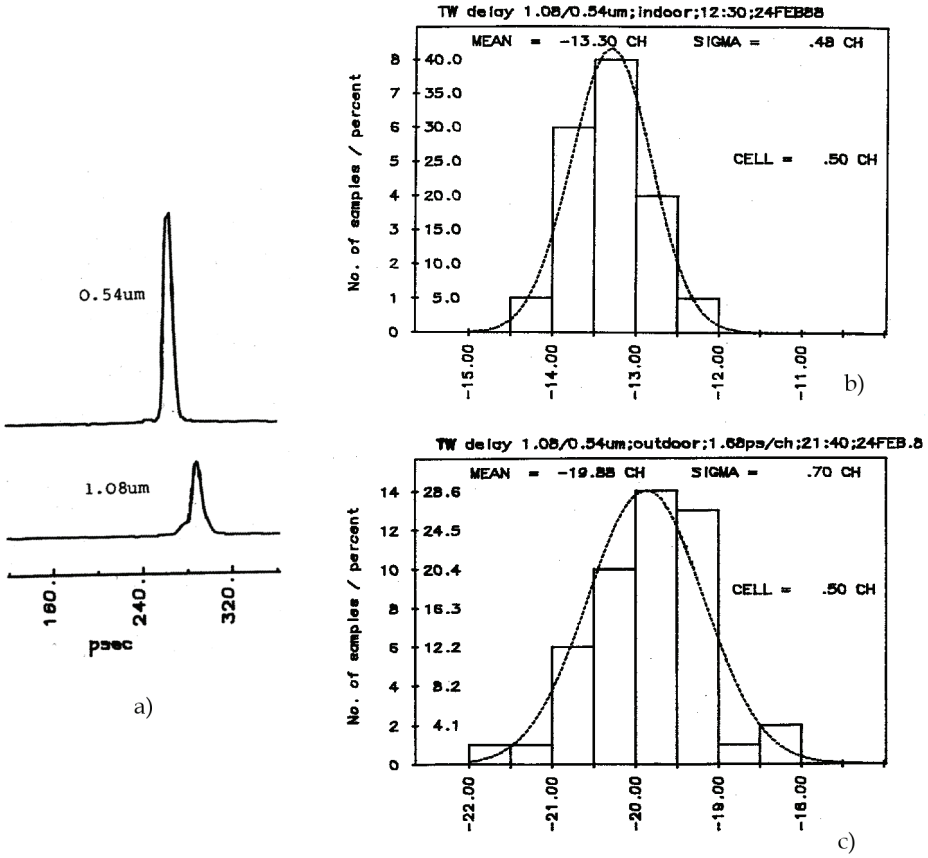

Fig. 1. Results of two wavelength ranging experiment (Hamal et al., 1988); pulse temporal profiles recorded by the linear streak camera (a) and delay histograms from indoor (b) and outdoor (c) ranging.

In contrast to astronomical imaging trough turbulent atmosphere, the picosecond pulse propagation and its distortion in a time domain has been studied just recently, once the picosecond lasers, detection and timing techniques became available. The effect has been observed for the first time (Hamal et al., 1988), when laser pulses 10 picoseconds long at the wavelength of 1079 nm and 539 nm were propagated different atmospheric path length two way, see figure 1. The pulses were transmitted simultaneously using passively mode locked Nd:YAP laser, part of the energy was converted to the second harmonic, pulses were propagated to the ground target formed by corner cube retroreflector at distances ranging from 1 to 200 meters. The returned optical signal was analysed using a linear streak camera. The streak camera together with image processing enabled to monitor simultaneously the returned signal beam direction fluctuations and fluctuations of the time interval between the two wavelength pulses. The timing resolution of the technique was high – typically 0.5 picosecond. The experiments showed the dependence of the pulse propagation delay fluctuation on both propagation distance and atmospheric fluctuation conditions. The

propagation delay fluctuations caused by the turbulent atmosphere were in the range of 0 to 1.5 ps for the propagation length 1 to 200 meter two way.
The experiment described above provided encouraging results, however, the technique (Hamal et al., 1988) was not suitable for routine measurements over longer baselines.

2. Theoretical models

The atmospheric turbulence – mixing of air of different temperatures, which causes random and rapidly changing fluctuations of air refractive index and hence unpredictable fluctuations from standard models of atmospheric range correction. We tried to estimate the atmospheric contribution to the ranging jitter using

1. an existing numerical modeling code (physical optics approach)
2. an analytical model developed by C. S. Gardner (geometric optics approach).

We used the commercial version of the General Laser Analysis and Design (GLAD) code (AOR, 2004). GLAD is an extensive program for modelling of diffractive propagation of light through various media and optical devices. The light is considered to be monochromatic and coherent (or partially coherent). The electromagnetic field in GLAD is described by its two-dimensional transversal distribution. Two arrays of complex numbers (one for each polarization state) represent the intensity and phase at each point in x and y axis. The propagation is done by the angular spectrum method. That means the field distribution is decomposed into a summation of plane waves, these plane waves are propagated individually and then resumed into resulting distribution. A user specifies a starting distribution at first and then applies aberrations, apertures, etc., and finally performs diffractive propagation of the distribution to some distance. At the end, the resulting distribution can be analysed. Using GLAD, we developed a model of atmospheric light propagation according to recommendations in GLAD Theoretical Description (AOR, 2004). It consists of alternating steps of random aberration and diffractive propagation applied to the initial plane wave.
After many attempts with different input parameters this model gives always pathlength RMS only several micrometers, i.e. negligible. What is even more surprising, the computed pathlength RMS does not significantly increase with L_0, as was expected from theory, although the wavefront size was always selected large enough ($10 \times L_0$) to model even the lowest-frequency aberrations. Therefore we have found this model not well describing the satellite laser ranging signal delay although the far field intensity profile has been modeled correctly. The origin of the problem has not been identified. The GLAD atmospheric model and its results correspond well to the "adaptive optics problem"; the corrections applied in adaptive optics are of the order of micrometers, just the values predicted by the model.
It is interesting discrepancy between wavefront shift necessary to correct the beam position and absolute propagation delay even of corrected laser beam.
In ref. (Gardner, 1976) derived analytical formulae that allow us to predict the turbulence--induced random pathlength fluctuations, directly for the case of satellite laser ranging, or generally for propagation delay. He also computed some concrete results and predicted that the RMS path deviations could reach millimeters, and at some extreme situations even several centimeters. However, Gardner used a very rough model of C_n^2 height dependence, which resulted in larger values of C_n^2 than are recently observed. We evaluated the Gardner's formulae using the recent model of C_n^2 height profile. For ground-to-space paths, we have selected the Hufnagel-Valley (Bass, 1992) model. This approach is predicting

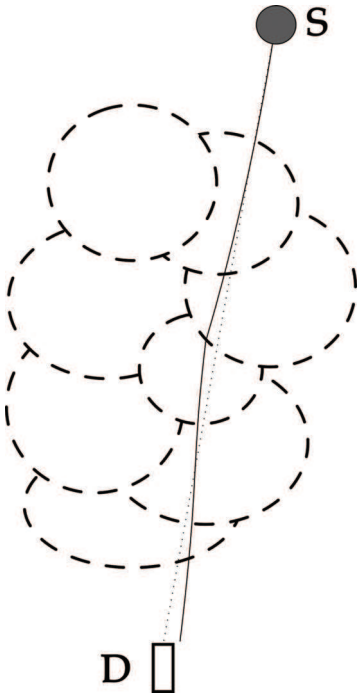

Fig. 2. The ideal (dotted) and real (solid) path of laser beam from source S (retro-reflector, start, artificial star) to detector.

realistic values of the atmospheric seeing induced range fluctuation of the order of millimeters.
It allows us to predict the turbulence-induced random fluctuations of optical path length, i.e. the turbulence-induced ranging jitter:

$$\sigma_{turb}^2 = 26.3 \cdot C_n^2(\xi = 0) \cdot L_0^{5/3} \cdot L_e \tag{1}$$

(eq. 20 in the Gardner's article, using the Greenwood-Tarazano spectral model of turbulence). σ_{turb} is the turbulence-induced ranging jitter, $C_n^2(\xi = 0)$ is turbulence strength at the beginning of the beam path (ξ is the distance from the observatory measured along the beam propagation path), L_0 is the turbulence outer scale (must be estimated) and L_e is effective pathlength given by

$$L_e = \frac{1}{C_n^2(\xi = 0)} \int_0^L C_n^2(\xi) d\xi \tag{2}$$

That means if we want to predict the turbulence-induced ranging jitter on a given path, we have to know integral of the turbulence strength C_n^2 along the path, and the outer scale L_0. The integral can be determined from measurement of astronomical seeing (FWHM of long exposure stellar image profile). To derive the relation between seeing and turbulence-induced ranging jitter, we used the two following relations

$$FWHM = \frac{\lambda}{r_0} \tag{3}$$

$$r_0 = 2.1 \cdot \left[1.46 \cdot k^2 \int_0^L C_n^2(\xi) \left(\frac{L-\xi}{L} \right)^{5/3} d\xi \right]^{-3/5} \tag{4}$$

where *FWHM* represents the value of seeing, r_0 is Fried's parameter, λ is wavelength of the seeing measurement, k is optical wavenumber equal to $2\pi/\lambda$, and L is one-way target distance. Using these relations, we were able to derive a relation allowing us to predict the turbulence-induced ranging jitter from the seeing measurement:

$$\sigma_{turb} = 1.28 \cdot L_0^{5/6} \cdot \lambda^{1/6} \cdot FWHM^{5/6} \tag{5}$$

for a slant path to space, and

$$\sigma_{turb} = 2.11 \cdot L_0^{5/6} \cdot \lambda^{1/6} \cdot FWHM^{5/6} \tag{6}$$

for a horizontal path. In the case of slant path to space, a star located at the same elevation as the ranging target can be used to measure the seeing FWHM. In the case of horizontal path, a ground-based point light source can be used, located in the same direction and the same distance as the ranging target (otherwise a correction for different distances must be applied).

3. Experimental setup

The experimental part was carried out at the Satellite Laser Ranging (SLR) station in Graz, Austria. The site is located 400 meters above the sea level. The laser ranging system consists of Nd:YAP diode-pumped laser with second harmonic generation (wavelength 532 nm, pulse width 8 ps), 10 cm transmitter telescope and 50 cm receiver telescope. The echo signal is detected by C-SPAD (Kirchner et al., 1997) (single photon avalanche detector with time walk compensation) and the time intervals are measured using event timer ET (Kirchner, Koidl, 2000). The laser operates at 2 kHz repetition rate, giving us sufficient sampling rate for the atmospheric influence investigation. The single shot precision of the whole system is 1 mm RMS (tested by ground target ranging). Such high repetition rate and ranging precision were necessary for the investigation of the turbulence influence, since the expected turbulence-induced jitter was of the order of one millimeter (maximum) and the fluctuation frequencies were expected up to 1 kHz.

We used three different types of laser ranging ground-based cube-corner retroreflector, a mobile retroreflector mounted on an airplane, and Earth orbiting satellites equipped by corner cube retroreflectors, see figure 3. In parallel, the atmospheric seeing was measured for a horizontal path of 4.3 km and a star in elevation close the satellite path. The standard Differential Image Motion Monitor (DIMM) technique (Beaumont, 1997) was employed.

The ground-based target was a cube-corner retroreflector mounted on a mast located 4.3 kilometers from the observatory. The laser beam path was horizontal and led over a hilly terrain covered with forests and meadows, with average height above the surface about 50 meters.

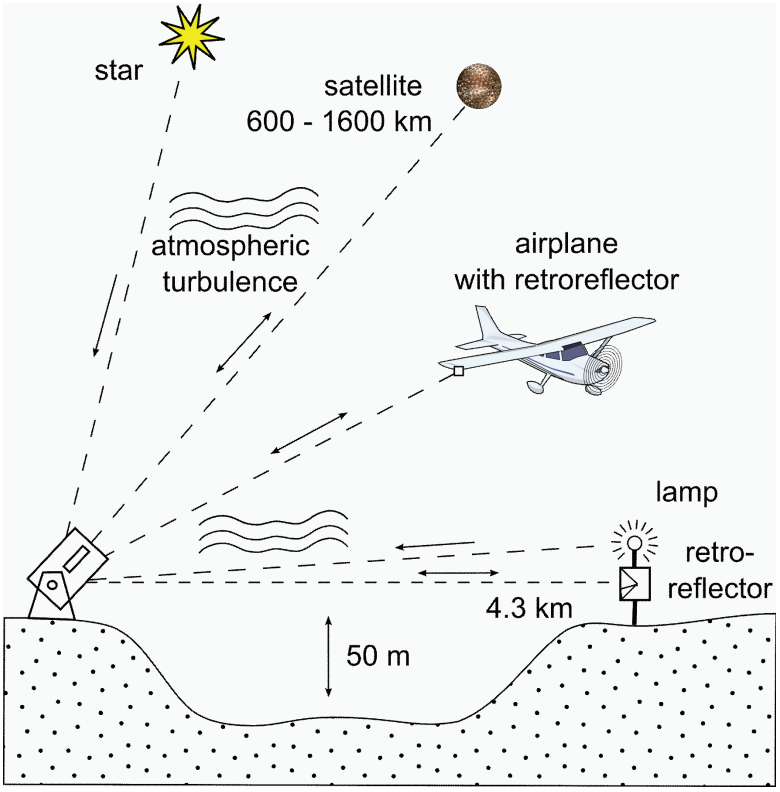

Fig. 3. Laser ranging to different targets and simultaneous seeing measurement to monitor atmospheric condition.

In the case of satellite ranging, we selected two satellites with low signature (not spreading the laser pulse in time) and high return energy, which leads to the best achievable ranging precision: ERS-2 and Envisat. We analyzed selected segments of their passes corresponding to different elevation above the horizon. Unfortunately, the laser ranging to an airplane based retro reflector did not provide sufficiently high quality data due to difficulties of optical tracking of such a target.

The typical measurement series consisted of hundred thousand of range measurements, normally distributed around the mean value. Since not every returns came from the retro (noise, prepulses), the typical sampling rate was around 1 kHz. This means the dataset covered about 100 seconds in time. However, the jitter of the measured range was sum of the instrumental jitter (stop detector, electronics etc.) and the turbulence-induced jitter:

$$\sigma^2 = \sigma_{inst}^2 + \sigma_{turb}^2 \tag{7}$$

Thus we had to extract the pure turbulence contribution σ^2_{turb} from the overall jitter σ (sigma denotes standard deviation). We took advantage of the knowledge that the instrumental jitter is completely random from shot to shot (behaves as white noise), whereas the atmospheric fluctuations are typically correlated over several neighboring shots (their time

spectrum is spread from 0 to some maximum frequency fmax, lower than the sampling frequency of 1 kHz).

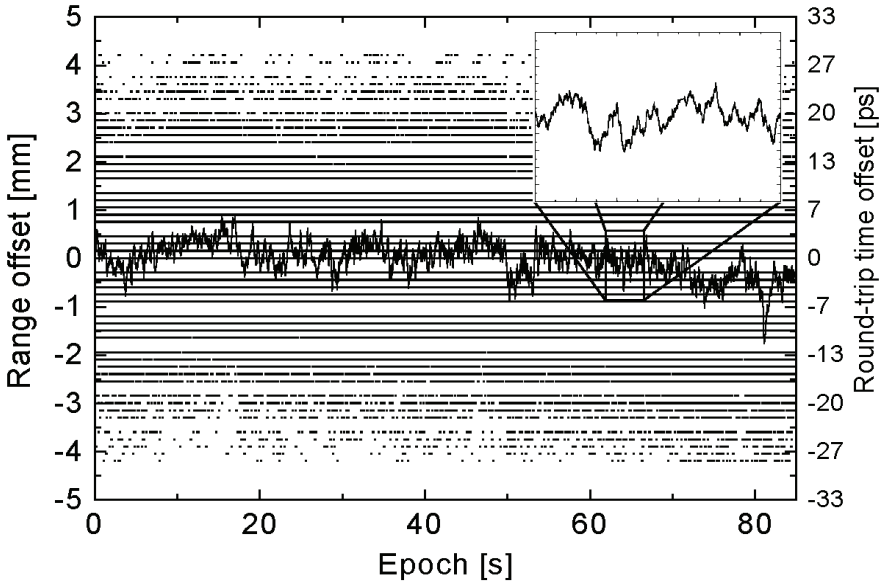

Fig. 4. Example of 4.3 km distant ground target ranging data (points) and 200-point moving average (line). Note the relatively fast turbulent fluctuations, and the long-term trend, later removed by polynomial fitting. The "pixelation" of orig. data is caused by a rounding of non-integer resolution of event timer – 1.2 ps.

If we compute averages from every N_a points of the dataset (normal points analogy from satellite laser ranging), the instrumental jitter will decrease root-square-of-N_a times, whereas the jitter of turbulence-induced fluctuations will remain the same, if the averaging interval will not be too wide. This is a similar situation to a sine wave combined with random noise – if the averaging interval will be shorter than approximately ¼ of the sine period, the sine wave will not be influenced by the averaging, whereas the random noise will be lowered. Now we can write an equation for the jitter σ_{avg} after the averaging:

$$\sigma_{avg}^2 = \left(\frac{\sigma_{inst}}{\sqrt{N_a}} \right)^2 + \sigma_{turb}^2 \tag{8}$$

now we have two equations (1) and (2) for two unknown variables σ_{turb} and σ_{inst}. Hence, the result will be

$$\sigma_{turb} = \sqrt{\frac{N_a \sigma_{turb}^2 - \sigma^2}{N_a - 1}} \tag{9}$$

This is the way, how to find out the pure turbulence contribution σ_{turb} to the overall ranging jitter σ.

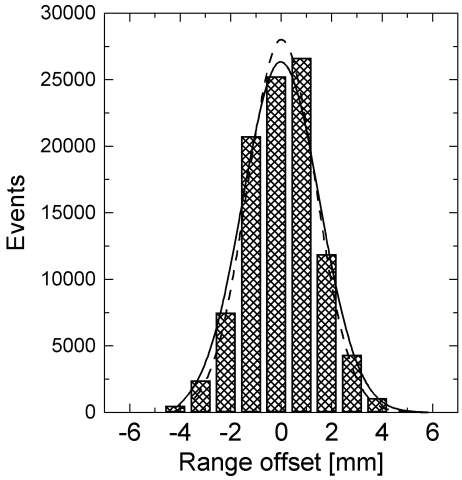

Fig. 5. Histogram from the dataset plotted at left figure 3. The solid line is gaussian fit for 3σ data editing criterion (RMS 1.4 mm), the dashed line is fit for 2.2σ criterion (RMS 1.2 mm).

However, there still remains the task to find out the maximum possible averaging interval Na. From above, the time interval corresponding to N_a must be shorter than approximately ¼ of the period of the fastest atmospheric fluctuation. Considering the spectral distribution of atmospheric fluctuations (Kral et al., 2006) the value $N_a = 3$ was used. The long-term trends in ranging data, caused by slow temperature and pressure changes during the measurement, see figure 4, were removed by polynomial fitting and computing of the residuals before further analysis, see figure 5. For the time spectrum see figure 6. Data was measured at SLR station Graz on May 10, 2004.

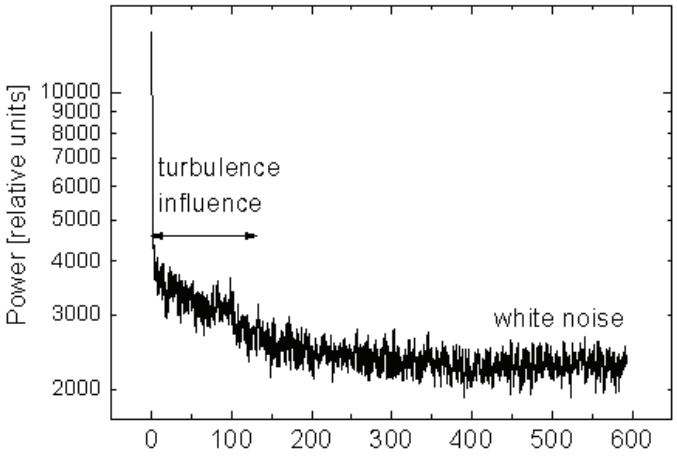

Fig. 6. Typical time spectrum of the fluctuations of measured range of the ground target. The turbulence significantly contributes at lower frequencies up to approx. 130 Hz. The sampling rate was 1.2 kHz. The same data like in figure 4.

4. Results

The computed values of the atmospheric turbulence contribution to the laser ranging fluctuation are summarized on figure 7 and 8. The figure 7 corresponds to the horizontal beam propagation, the figure 8 corresponds to the slant path to space for elevation range between 15 and 65 degrees. The measured values – filled squares – are plotted over the theoretical curves computed for different values of the outer scale parameter L_0.

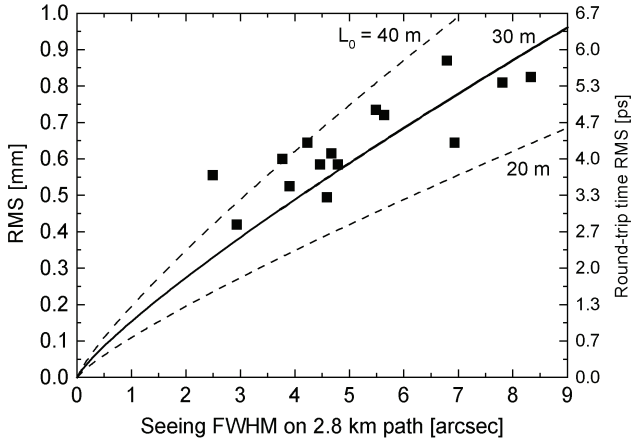

Fig. 7: The turbulence-induced ranging jitter as a function of turbulence strength (measured by the seeing). The graph was constructed from measurements of the 4.3 km distant ground target (horizontal path), taken under various meteorological conditions.

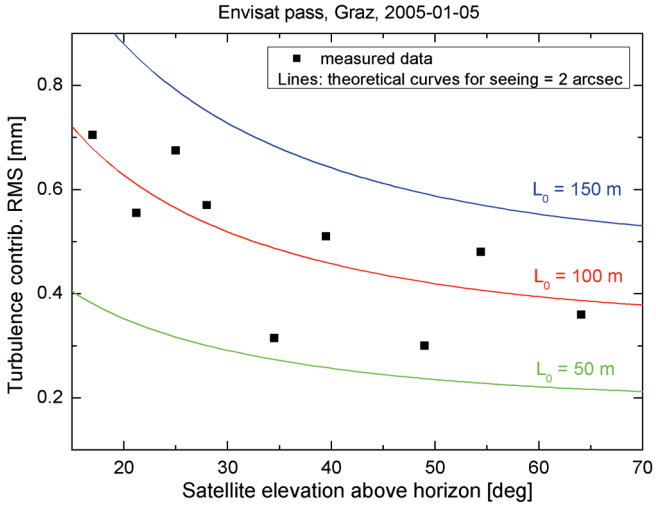

Fig. 8. The turbulence-induced ranging jitter as a function of satellite elevation. The graph was constructed from satellite measurements by slant path to space.

From these two figures one can conclude, that the values of 30 meters and 100 meters fit best the measured values for the horizontal and slant path to space respectively. This is a first experimental determination of the outer scale parameter. The outer scale L_0 is key to measure, and still not well understood. By measurement of seeing parameter together with determination of the laser ranging jitter from satellite laser ranging data, the outer scale L_0 can be determined. However, to carry out such a measurement, the high repetition rate laser ranging system (2 kHz rate is a minimum) with (sub) millimeter single shot instrumental ranging precision is required. These are quite challenging system requirements.

5. Future outlook

As it was described in the previous chapters, the instrumental precision of the laser ranging system is a key to the atmospheric turbulence influence on the laser pulse propagation studies. Recently, new technologies are emerging and becoming available, which will improve the instrumental resolution of the laser ranging chain, namely new timing systems and improved echo signal detectors.

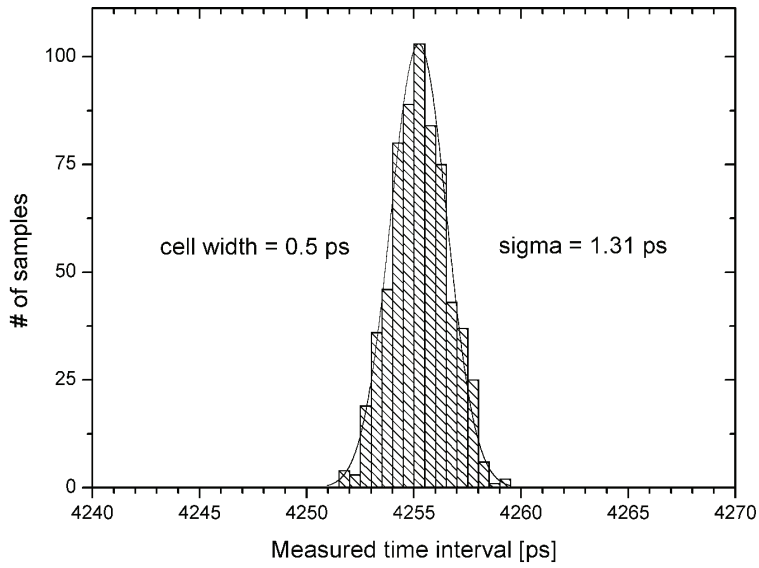

Fig. 9. N-PET timing device temporal resolution, two channel cable delay test.

The new sub-picosecond resolution event timing (N-PET) system has been developed by our group (Panek & Prochazka, 2007). It provides the single shot timing resolution of 920 femtoseconds per channel, see figure 9, and excellent timing linearity and temporal stability, see figure 10, of the order of hundreds of femtoseconds.

This novel timing system has been tested at the laser ranging facility in Graz and provided better instrumental resolution of the system along with ranging data distribution closed to the normal one.

The second key contributor to the instrumental resolution limitation is the echo signal detector. The avalanche photodiode based detector operating in the single and multi-photon

counting regime is routinely used (Prochazka et al., 2004). Recent achievements in the detector chip signal processing (Blazej & Prochazka, 2008) will enable to lower the error correlated with the signal strength fluctuation and hence further improve the instrumental resolution namely for ranging to space targets.

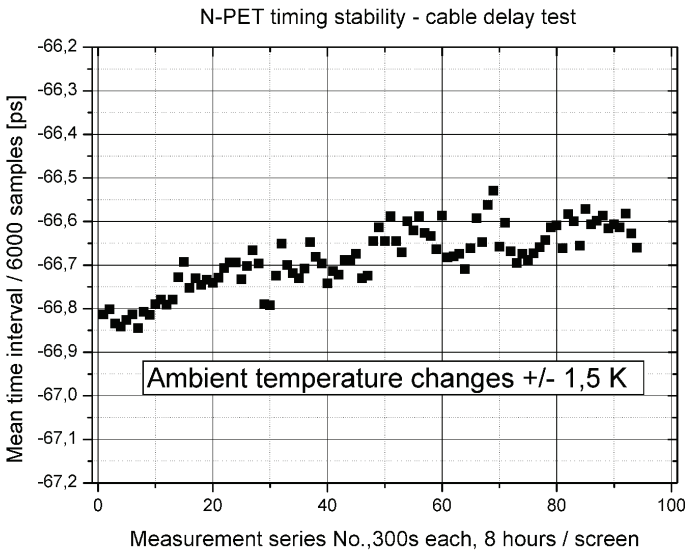

Fig. 10. N-PET timing device temporal stability.

6. Conclusion

We are presenting the results of the studies related to propagation of ultrashort optical pulse through the turbulent atmosphere. Three independent types of path configurations have been studied: horizontal path, slant path at elevation 10 – 80 degrees to a flying target and slant path from ground to space. The correlation of the atmospheric turbulence with the propagation delay fluctuation was measured. The appropriate theoretical model was found and matched to the experimental results. The entirely different approach in comparison to adaptive optics was developed to describe the effect. The experiments described enabled us for the first time to determine the outer scale parameter L_0 on the basis of direct measurement. The recent achievements in the field of pulsed lasers, fast optical detectors and timing systems enable us to resolve the effects of propagation differences monitoring on the level of units of picosecond propagation time. Additionally, new techniques of optical receivers signal processing give a way to distinguish the atmospheric fluctuations contribution from the energy dependent detection delay effects.

7. Acknowledgement

Authors would like to express their thanks to Georg Kirchner and Franz Koidl, Graz SLR station. This research has been supported by the Research framework of Czech Ministry of Education № MSM6840770015.

8. References

Applied Optics Research (AOR), (2004). *GLAD Users Guide*, ver. 4.5, Applied Optics Research, Washington.

Applied Optics Research (AOR), (2004). *GLAD Theoretical Description*, ver. 4.5, Applied Optics Research, Washington.

Bass, M. (1992). *Handbook of Optics*, McGraw-Hill Professional, ISBN 978-0070477407, vol. 1, Chapter 44.

Beaumont, H. et al. (1997). Image quality and seeing measurements for long horizontal overwater propagation. *Pure Applied Optics,* Vol. 6, pp. (15–30), ISSN 0963-9659.

Blazej, J., Prochazka, I., (2008). Photon number resolving detector in picosecond laser ranging and time transfer in space, *Technical Digest «Modern problems of laser physics»*, p.183., Novosibirsk, Russia, August 24 – 30 2008, SB RAS, Novosibirsk, Russia.

Degnan, J. J. (1993). Millimeter Accuracy Satellite Laser Ranging: A Review, *Contributions of Space Geodynamics: Technology*, D. E. Smith and D. L. Turcotte (Eds.), AGU Geodynamics Series, Vol. 25, pp. (133-162).
[online] <http://ilrs.gsfc.nasa.gov/reports/degnan/index.html>

Gardner, C. S. (1976). Effects of random path fluctuations on the accuracy of laser ranging systems, *Applied Optics*, Vol. 15, No. 10, p. 2539, ISSN 0003-6935.

Hamal, K., Prochazka, I., Schelev, M., Lozovoi, V., Postovalov, V. (1988). Femtosecond Two wavelength Laser Ranging to a Ground Target, Proceedings of SPIE Vol. 1032, pp. 453-456, ISBN 9780819400673, Xian, People's Republic of China, August 28 – September 2 1988, SPIE, Bellingham, WA, USA.

Kirchner, G., Koidl, F., Blazej, J., Hamal, K., Prochazka, I. (1997). Time-walk-compensated SPAD: multiple-photon versus single-photon operation, *Proceedings of SPIE Vol. 3218*, p. 106. ISBN 9780819426505, London, UK, September 24 – 26 1997, SPIE, Bellingham, WA, USA.

Kirchner, G., Koidl, F. (2000). Graz Event Timing system E. T., *Proceedings of the 12th International Workshop on Laser Ranging*, Matera, Italy, November 13 – 17, 2000 [online]
<http://geodaf.mt.asi.it/html_old/news/iwlr/Kirchner_et_Koidl_ET.pdf>, ILRS, USA.

Kral, L., et al., (2006). Random fluctuations of optical signal path delay in the atmosphere, *Proceedings of SPIE 6364*, p. 0M, ISBN: 9780819464590, Stockholm, Sweden, 11 September 2006, SPIE, Bellingham, WA, USA.

Niell, A. E. (1996). Global mapping functions for the atmosphere delay at radio wavelengths, *Journal of Geophysical Research,* Vol. 101, No. B2, pp. (3227-3246), ISSN 0148-0227.

Panek, P., Prochazka, I. (2007). Time interval measurement device based on surface acoustic wave filter excitation, providing 1 ps precision and stability, *Review of Scientific Instruments*, Vol. 78, No. 9, pp. (78-81), ISSN 0034-6748.

Prochazka, I., Hamal, K., Sopko, B. (2004). Recent Achievements in Single Photon Detectors and Their Applications, *Journal of Modern Optics,* Vol. 51, No. 9, pp. (1298-1313), ISSN 0950-0340.

Roddier, F. (1998), Curvature sensing and compensation: a new concept in adaptive optics, *Applied Optics,* Vol. 27, No. 7, p. 1223, ISSN 0003-6935.

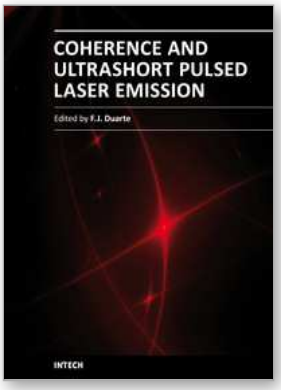

Coherence and Ultrashort Pulse Laser Emission

Edited by Dr. F. J. Duarte

ISBN 978-953-307-242-5
Hard cover, 688 pages
Publisher InTech
Published online 30, November, 2010
Published in print edition November, 2010

In this volume, recent contributions on coherence provide a useful perspective on the diversity of various coherent sources of emission and coherent related phenomena of current interest. These papers provide a preamble for a larger collection of contributions on ultrashort pulse laser generation and ultrashort pulse laser phenomena. Papers on ultrashort pulse phenomena include works on few cycle pulses, high-power generation, propagation in various media, to various applications of current interest. Undoubtedly, Coherence and Ultrashort Pulse Emission offers a rich and practical perspective on this rapidly evolving field.

How to reference

In order to correctly reference this scholarly work, feel free to copy and paste the following:

Ivan Prochazka, Lukas Kral and Josef Blazej (2010). Picosecond Laser Pulse Distortion by Propagation through a Turbulent Atmosphere, Coherence and Ultrashort Pulse Laser Emission, Dr. F. J. Duarte (Ed.), ISBN: 978-953-307-242-5, InTech, Available from: http://www.intechopen.com/books/coherence-and-ultrashort-pulse-laser-emission/picosecond-laser-pulse-distortion-by-propagation-through-a-turbulent-atmosphere

INTECH
open science | open minds

InTech Europe
University Campus STeP Ri
Slavka Krautzeka 83/A
51000 Rijeka, Croatia
Phone: +385 (51) 770 447
Fax: +385 (51) 686 166
www.intechopen.com

InTech China
Unit 405, Office Block, Hotel Equatorial Shanghai
No.65, Yan An Road (West), Shanghai, 200040, China
中国上海市延安西路65号上海国际贵都大饭店办公楼405单元
Phone: +86-21-62489820
Fax: +86-21-62489821